e Q q measurements in the X, 1g, O + g and B state of I2: A test of the electronic molecular eigenfunctions

R. Bacis, M. Broyer, S. Churassy, J. Vergès, and J. Vigué

Citation: The Journal of Chemical Physics **73**, 2641 (1980); doi: 10.1063/1.440477
View online: http://dx.doi.org/10.1063/1.440477
View Table of Contents: http://scitation.aip.org/content/aip/journal/jcp/73/6?ver=pdfcov
Published by the AIP Publishing

eQq measurements in the *X*, $1g$, O_g^+ and *B* state of I_2: A test of the electronic molecular eigenfunctions

R. Bacis

Laboratoire de Spectrométrie Ionique et Moléculaire, Université Claude Bernard Lyon I 43, Boulevard du 11 Novembre 1918, 69622 Villeurbanne, (France)

M. Broyer

Laboratoire de Spectroscopie Hertzienne de l'Ecole Normale Supérieure 24, rue Lhomond 75005 Paris, (France)

S. Churassy

Laboratoire de Spectrométrie Ionique et Moléculaire, Université Claude Bernard Lyon I 43, Boulevard du 11 Novembre 1918, 69622 Villeurbanne, (France)

J. Vergès

Laboratoire Aimé Cotton C.N.R.S. II Bâtiment 505, 91405 Orsay, (France)

J. Vigué

Laboratoire de Spectroscopie Hertzienne de l'Ecole Normale Supérieure 24, rue Lhomond 75005 Paris, (France)
(Received 1 April 1980; accepted 28 May 1980)

The laser induced fluorescence spectra of I_2 recorded with a high resolution Fourier Transform Spectrometer (LIF–FTS) enables us to measure the hyperfine parameters *eQq* in three states of I_2; the *X* state and the recently discovered 1_g and O_g^+ states. For each state *eQq* is obtained in various vibrational levels and especially in the *X* state, we obtain the complete variation curve of *eQq* as a function of the vibrational energy. All these results and some other ones available in the literature are interpreted using LCAO eigenfunctions for short internuclear distance and separated atom basis set near the dissociation limit. The agreement with the experimental results is very good and it is possible to observe the transition between the two basis sets.

I. INTRODUCTION

The quadrupolar electric coupling constant *eQq* is known for many molecules in their ground state. Up until now except in the I_2 *B* state, few results have been published concerning the excited electronic states and the variation of the *eQq* constant as a function of the vibrational energy in a given electronic state. The recent development of laser induced fluorescence spectra recorded with a high resolution Fourier transform spectrometer (LIF–FTS) has shown the high capabilities of this technique.[1,12] In this paper we show how a precise line shape analysis of LIF–FTS spectra permits us to measure the hyperfine structure in three states of iodine: $X\,^1\Sigma_g^+$ and two recently discovered 1_g and O_g^+ states.[1] Especially in the *X* state, the *eQq* hyperfine constant is obtained as a function of the vibrational energy from the bottom of the potential well up to levels close to the dissociation limit. All these hyperfine measurements involve transitions extending from 20 000 to 7500 cm^{-1}.

All these results and some others available in the literature may be interpreted with the help of *ab initio* calculations (i.e., referred to the experimental atomic values). At relatively short internuclear distance we use the usual LCAO eigenfunction. Near the dissociation limit, we use the Separated Atom basis set which has been introduced[2] by two of us to calculate the perturbation of the *B* state at large internuclear distance. As a consequence of these features, the *eQq* measurements may be considered as a probe of the electronic eigenfunctions. For example, in the *X* state we are able to check the internuclear distance from which the separated Atom basis set is a good approximation.

In the two first sections of our paper, we explain how the *eQq* constant can be calculated theoretically. In the two last sections we give our experimental results referring also to previous measurements and then compare them with the present theory.

II. *eQq* CALCULATIONS IN THE LCAO APPROXIMATION

The nuclear quadrupole moment *Q* is a property of the nucleus and its value is available in the literature for a large number of nuclei. The quantity *e* is the proton charge, *q* is the average of the electric field gradient created at the position of the nucleus and depends upon molecular eigenfunctions. For a diatomic homonuclear molecule in an electronic state denoted as $^{2S+1}\Lambda_\Omega$, *q* may be written

$$q = 2\langle S\Lambda\Omega|\sum_e V_0^2(a, e)|S\Lambda\Omega\rangle$$

$$= 2\langle S\Lambda\Omega|\sum_e V_0^2(b, e)|S\Lambda\Omega\rangle\,, \qquad (1)$$

where *a* and *b* are the two nuclei, and the summation extends over all the electrons, with

$$V_q^2(a, e) = \left(\frac{4\pi}{5}\right)^{1/2} \frac{-e}{4\pi\epsilon_0 r_{ae}^3}\, Y_q^2(\theta_{ae}, \phi_{ae})\,, \qquad (2)$$

θ_{ae} and ϕ_{ae} being the angular coordinates of the vector $\mathbf{r}_{ae}$.

 0021-9606/80/182641-10$01.00

Theoretical calculations of q were already performed many years ago to interpret numerous results obtained for the ground states of molecules. The usual method is based on LCAO eigenfunctions. This method is explained in details for example in *Microwave Spectroscopy*[3] of Townes and Schawlow or *Microwave Molecular Spectra*[4] of Gordy and Cook. We recall only the final result:

If the molecular orbitals are expressed as a linear combination of atomic orbitals ψ^a_{nlm} and ψ^b_{nlm} of atoms a and b, $\psi = (1/\sqrt{2})(\psi^a_{nlm} \pm \psi^b_{nlm})$ for a diatomic homonuclear molecule, then q may be calculated by the formula

$$q = \sum_{\substack{\text{valence} \\ \text{electrons}}} \frac{1}{2} q_{nlm} . \tag{3}$$

The ψ^a_{nlm} are the atomic wave functions of atom a with the usual definitions for the atomic quantum numbers n, l, m. The axis of quantization is the internuclear axis:

$$q_{nlm} = 2 \langle nlm | V^2_0(a, e) | nlm \rangle . \tag{4}$$

q_{nlm} may be known from the atomic quadrupole coupling constant.

In formula (3), the electric field gradient created by the electrons of atom b at the position of atom a is neglected. This approximation is reasonable because q contains the factor $1/r^3_{ae}$, which is very weak for an electron in an orbital centered on nucleus b and is mainly cancelled by the charge of the other nuclei.

In the I_2 molecule, there are five valence electrons for which $n=5$, $l=1$, $m=0$ in σ orbitals and $m=1$ in π orbitals. For the atom ^{127}I,[3-5]

$$eQq_{510} = 2292.7 \text{ MHz}$$

and

$$eQq_{511} = eQq_{51-1} = -\tfrac{1}{2} eQq_{510} .$$

To calculate eQq in a given electronic state of I_2, we have to know the LCAO configuration of this state. For example the ground $X\,^1\Sigma^+_g$ state belongs[6] to the σ^2_g, π^4_u, π^4_g, σ^0_u configuration. Therefore we must add the contribution of two $(5p\sigma)$ orbitals for which $m=0$, and eight $(5p\pi)$ orbitals for which $|m|=1$:

$$q_X = \tfrac{1}{2}(2q_{510} + 8q_{511})$$

and

$$eQq_X = -2293 \text{ MHz} .$$

The eQq values of the states $X\,^1\Sigma^+_g$, $^3\Pi_{O^+_g}$, $^3\Pi_{1_g}$, and $B\,^3\Pi_{O^+_u}$ may be calculated by the same method. The results are given in Table I.

A remark must be made concerning the $^3\Pi_{1_g}$ state. The matrix elements of the electric quadrupole hyperfine Hamiltonian H_Q have not exactly the same expression for an $\Omega=1$ state as for an $\Omega=0$ state. Indeed the eigenfunctions for an $\Omega=1$ state are $(1/\sqrt{2})(|\Omega=\pm1\, v J M_J\rangle + \epsilon |\Omega=1\, v J M_J\rangle)$ with $\epsilon=\pm1$, and H_Q may couple $\Omega=-1$ states to $\Omega=+1$ states because the internuclear axis is not a symmetry axis for H_Q.

In fact, the matrix elements of H_Q in an $\Omega=1$ state are exactly the same as in $\Omega=0$ states,[7] if we replace the usual eQq by an $(eQq)_{\text{eff}}$ defined by

$$(eQq)_{\text{eff}} = eQq_1[1 - 3/J(J+1)] - \epsilon(\tfrac{1}{2}\sqrt{6})\, eQq_{\perp 1} , \tag{5}$$

where

$$q_1 = 2 \langle S\Lambda\Omega = 1 | \sum_e V^2_0(a, e) | S\Lambda\Omega = 1 \rangle \tag{6}$$

and

$$q_{\perp 1} = 2 \langle S\Lambda\Omega = 1 | \sum_e V^2_2(a, e) | S\Lambda\Omega = -1 \rangle . \tag{7}$$

For the $^3\Pi_g$ state, q_{1_g} may be calculated by formula (3). The calculation of $q_{\perp 1_g}$ is a little more complicated, the details are given in Appendix A and the final result is quoted in Table I. $(eQq)^{1_g}_{\text{eff}}$ may be written

$$(eQq)^{1_g}_{\text{eff}} = -573 \text{ MHz}\,[1 - 3/J(J+1) - 3\epsilon] . \tag{8}$$

All these LCAO calculations are generally valid when the atoms are not too far from one another. If the internuclear distance is very large, the molecule may be approximately conceived as two separated atoms. In a recent paper, Vigué *et al.*[2] have shown that the electronic eigenfunction of the I_2 molecule in a level close to the dissociation limit may be approximated by symmetrized products of two ^{127}I atom eigenfunctions. We now want to calculate eQq in this basis set for the four I_2 states under consideration.

TABLE I. eQq theoretical values in the two basis sets: LCAO and separated atoms (SA).

	LCAO configuration $\sigma_g\,\pi_u\,\pi_g\,\sigma_u$	eQq From LCAO (MHz)	eQq From SA (MHz)
$X\,^1\Sigma^+_g$	2440	$eQq_X = -2293$	$eQq_X = -1146$
$^3\Sigma^-_{O^+_g}$	2422	$eQq_{O^+_g} = +1146$	$eQq_{O^+_g} = +1146$
		$eQq_{1_g} = -573$	$eQq_{1_g} = 0$
$^3\Pi_{1_g}$	2341	$= -1404$ $eQq_{\perp 1_g} = \sqrt{6}\; eQq_{1_g}$	$eQq_{\perp 1_g} = 0$
$B\,^3\Pi_{O^+_u}$	2431	$eQq_B = -573$	$eQq_B = -573$

III. eQq CALCULATIONS IN THE SEPARATED ATOM BASIS SET

In this basis set, the usual quantum numbers Λ and S are no more defined, only Ω is a good quantum number: it is a Hund case c basis set. The electronic eigenfunctions are found from the atomic states of the dissociation products, using the proper symmetrization.[8]

The B state dissociates into one atom in the $^2P_{3/2}$ state and one atom in a $^2P_{1/2}$ state

$$|B\,O^+_u\rangle = \tfrac{1}{2}\left(\left|\tfrac{3}{2}\tfrac{1}{2}\right\rangle_a \left|\tfrac{1}{2}-\tfrac{1}{2}\right\rangle_b + \left|\tfrac{1}{2}-\tfrac{1}{2}\right\rangle_a \left|\tfrac{3}{2}\tfrac{1}{2}\right\rangle_b + \left|\tfrac{3}{2}-\tfrac{1}{2}\right\rangle_a \left|\tfrac{1}{2}\tfrac{1}{2}\right\rangle_b + \left|\tfrac{1}{2}\tfrac{1}{2}\right\rangle_a \left|\tfrac{3}{2}-\tfrac{1}{2}\right\rangle_b\right) . \tag{9}$$

The three other states 1_g, XO^+_g, and O^+_g dissociate into two iodine atoms in the $^2P_{3/2}$ state

$$|1_g\rangle = (1/\sqrt{2})\left(\left|\tfrac{3}{2}\tfrac{3}{2}\right\rangle_a \left|\tfrac{3}{2}-\tfrac{1}{2}\right\rangle_b - \left|\tfrac{3}{2}-\tfrac{1}{2}\right\rangle_a \left|\tfrac{3}{2}\tfrac{3}{2}\right\rangle_b\right) , \tag{10}$$

$$|XO^+_g\rangle = (1/\sqrt{2})\left(\left|\tfrac{3}{2}\tfrac{1}{2}\right\rangle_a \left|\tfrac{3}{2}-\tfrac{1}{2}\right\rangle_b - \left|\tfrac{3}{2}-\tfrac{1}{2}\right\rangle_a \left|\tfrac{3}{2}\tfrac{1}{2}\right\rangle_b\right) , \tag{11}$$

$$|O_g^+\rangle = (1/\sqrt{2})\left(\left|\tfrac{3}{2}\,\tfrac{3}{2}\right\rangle_a \left|\tfrac{3}{2}\,-\tfrac{3}{2}\right\rangle_b - \left|\tfrac{3}{2}\,-\tfrac{3}{2}\right\rangle_a \left|\tfrac{3}{2}\,\tfrac{3}{2}\right\rangle_b\right) . \quad (12)$$

Since there are two O_g^+ states, it is not clear *a priori* why expression (11) corresponds to the X state. An argument may be found in the original paper of Mulliken[9]; the $^3\Sigma_{O_g^+}^-$ state has the following configuration in term of separated atomic orbitals: $\sigma^2\pi^3$ for atom a and $\sigma^2\pi^3$ for atom b; therefore, $M_L = \pm 1$ for atoms a and b just as in atomic states $|\tfrac{3}{2}\,\tfrac{3}{2}\rangle$ and $|\tfrac{3}{2}\,-\tfrac{3}{2}\rangle$. Another argument is related to the bonding character of states (11) and (12): under some conditions the $5p^5$ configuration of iodine atom is equivalent to a $5p$ configuration through the Racah teorem. A strongly bond state as the X state requires an important overlap of the atomic orbitals. This overlap is small for $m_L = \pm 1$ states and large for $m_L = 0$ states which are absent in expression (12).

From formulas (9) to (12), the q values of the various molecular I_2 states may easily be related to the atomic $q_{3/2}$ value in the $^2P_{3/2}$ state, q being equal to zero in the $^2P_{1/2}$ state for symmetry reasons. We give, for example, the q derivation in the X state

$$q_X = 2\langle X O_g^+ | \sum_e V_0^2(a, e) | X O_g^+\rangle ,$$
$$q_X = 2_a\langle \tfrac{3}{2}\,\tfrac{1}{2} | \sum_e V_0^2(a, e) | \tfrac{3}{2}\,\tfrac{1}{2}\rangle_a . \quad (13)$$

Then we use the Wigner–Eckart theorem[10]:

$$q_X = (-1)^{3/2-1/2} \begin{pmatrix} \tfrac{3}{2} & 2 & \tfrac{3}{2} \\ -\tfrac{1}{2} & 0 & \tfrac{1}{2} \end{pmatrix} \times \langle {}^2P_{3/2} \| 2 \sum_e V_0^2(a, e) \| {}^2P_{3/2}\rangle . \quad (14)$$

The $3j$ symbol is tabulated and the reduced matrix element may be related to $q_{3/2}$ by standard method. Finally, we obtain

$$q_X = -q_{3/2} ;$$

and in the same way

$$q_{O_g^+} = +q_{3/2} , \qquad q_B = -\tfrac{1}{2} q_{3/2} ,$$
$$q_{1_g} = 0 , \qquad q_{11_g} = 0 .$$

The corresponding eQq values are reported in Table I. We must now compare these theoretical results with the experiment.

IV. EXPERIMENTS

The measurements were made from laser induced fluorescence spectra recorded with a high resolution Fourier transform spectrometer (LIF–FTS). This technique was first developed from the iodine molecule fluorescence[1,11] and extended to other molecules.[12]

Various iodine fluorescence spectra have been recorded from Ar^+ and Kr^+ exciting laser lines. This has allowed the long range analysis of the X state and the discovery of the bonding character of the 1_g and O_g^+ states at large internuclear distance.[1,11,13] The whole fluorescence spectrum is covering the range from 20 000 to 7000 cm^{-1}. In order to have a very good signal to noise ratio (SNR) for the main fluorescence lines various filters were used so that this full range is obtained from five separate records.

The line shape analysis has been made in two regions; one as close as possible of the dissociation limit from 514.5 nm (Table II) and 501.7 nm (Table III) laser lines; the other are in the range where eQq'' of the X state is

TABLE II. eQq_X measurements performed with the 514.5 nm excitation laser line. For each v'' vibrational level studied in this work the fluorescence lines were R (11), $R(15)$, P (13), P (17) (emission in the 7300–8050 cm^{-1} range). These results were obtained using the best eqQ_B value in $v' = 43$: $eQq_B = -558.6$ MHz (Ref. 14). The results from Refs. 13 and 16 are corrected taking into account this best eQq_B value. The given error is an estimate of the standard deviation (see text).

v	r_1 [a]	r_2 [a]	P_2	$E_{Dis} - E_v$ (cm^{-1})	eQq (this work) (MHz)	(other results)	eQq (r_2) (MHz)
0	2.62	2.72	0.5	12 440.09		−2452[b]	−2452
11	2.46	2.96	0.467	10 162.45		−2455 ± 2[c]	−2455
42	2.33	3.39	0.65	4664.43		−2364 ± 1	−2312
62	2.30	3.74	0.751	2 056.60		−2128 ± 1[d]	−2018
73	2.28	4.04	0.825	1 058.03	−1918 ± 40		−1803
74	2.28	4.07	0.832	984.82	−1861 ± 30		−1740
75	2.28	4.11	0.839	914.61	−1852 ± 70		−1734
76	2.28	4.14	0.846	847.40	−1805 ± 15		−1692
77	2.28	4.18	0.854	783.15	−1795 ± 40		−1681
78	2.28	4.22	0.860	721.87	−1734 ± 15		−1617
79	2.28	4.27	0.867	663.54	−1701 ± 15	−1692 ± 1[d]	−1585
80	2.28	4.31	0.874	608.12	−1632 ± 30		−1530
81	2.28	4.36	0.881	555.60	−1638 ± 15	−1629 ± 3[d]	−1519
82	2.28	4.41	0.887	505.94	−1604 ± 15		−1495
83	2.27	4.46	0.894	459.11	−1557 ± 15	−1556 ± 1[e]	−1449
84	2.27	4.52	0.900	415.07	−1520 ± 30		−1417
85	2.27	4.58	0.907	373.77	−1480 ± 20		−1379
86	2.27	4.64	0.913	335.19	−1469 ± 50		−1374

[a] Taken from Ref. 11.
[b] Taken from Refs. 14 and 17.
[c] Taken from Ref. 16.
[d] Taken from Ref. 13.
[e] Taken from Ref. 15.

TABLE III. eQq_X measurements performed with the 501.7 nm excitation laser line. The measurements were made from two different records (resolution limit 0.0060 and 0.0072 cm^{-1}) covering the 7825–7490 cm^{-1} range. The given error is the R.M.S. deviation from 8 measurements obtained with the R (10) and P (12) (from $v'=61$) and R (26) and P (28) ($v'=62$). eqQ_B was set to −569 MHz (Ref. 14).

v''	eQq_X (MHz)	$E_{Dis}-E_v$ (cm^{-1})
82	−1740 ± 150	505, 94
83	−1605 ± 70	459, 11
84	−1495 ± 50	415, 07
86	−1473 ± 60	335, 19
87	−1148 ± 60	299, 25
88	−1405 ± 30	265, 95
89	−1279 ± 60	235, 21
91	−1268 ± 110	181, 27
92	−1124 ± 40	157, 93
93	−947 ± 50	136, 91
94	−1068 ± 20	118, 05
95	−940 ± 70	101, 20
96	−949 ± 110	86, 17
98	< −970	60, 90
100	−1500 ± 400	41, 04
101	−1635 ± 150	33, 99
102	−1480 ± 140	26, 10
103	−1510 ± 120	20, 08
104	−1600 ± 100	15, 12
105	−1640 ± 90	11, 02
106	−1550 ± 100	7, 65
107	−1690 ± 120	5, 20

beginning to decrease (in absolute value) from 530.8 nm Kr^+ line (Table IV).

In these Fourier transform experiments, the apparatus function is about 0.0007 cm^{-1} (210 MHz), while the observed fluorescence linewidth varies from 0.010 to 0.020 cm^{-1} and exhibits a small but unambiguous asymmetry [see Fig. 1(b)]. Indeed this linewidth and this asymmetry result from the hyperfine structure convoluted with the Doppler width, and then depend upon the temperature T and the difference between the hyperfine parameters of the excited and ground states. In most studies cases the only important hyperfine parameter is eQq in both excited and lower states and the related linewidth is proportional to $\Delta eQq = eQq' - eQq''$. Since the hyperfine parameters of the various excited vibrational levels of the B state ($v'=32$, 43, 62) are known[14,22] and that the hyperfine structure in the various ground states is due mainly to the electric quadrupole term eQq'', the fluorescence linewidth depends only upon two unknown parameters: the eQq'' constant in the ground state and the temperature T of the molecules in the cell which defines the Doppler width. T is not the room temperature because the power of the laser line 514.5 nm is 7 W and an important part of this energy heats the molecule through collision energy transfer in the ground state or absorption via the continuum.

Therefore the line profile may be calculated as a function of the two parameters eQq'' and T. Moreover, the temperature T is the same for all the lines observed in a given run. For each set of eQq'' and T values, we have computed the red half-width at half-maximum (HWHM) and the violet HWHM of each line. These two HWHM are compared with the experimental profiles.

For instance the temperature T corresponding to the 514.5 nm excitation was measured from a spectrum covering the 7000–8000 cm^{-1} range where a long time record (~10 h) gave a very high signal to noise ratio (~5000) for the main fluorescence lines, despite a 0.0072 cm^{-1} resolution limit.

This temperature T is determined through the more intense transitions B–X corresponding to $v''=74$, 76, 79, 81, and 83: for a given line and a given temperature, there is one eQq'' value which gives the experimental full width at half-maximum (FWHM) of the lines, but not necessarily the correct asymmetry. By varying the temperature, we now obtain one set of T and eQq'' values which reproduces the two experimental HWHM. The two parameters T and eQq'' are poorly correlated because

TABLE IV. eQq_X measurements performed with the 530.8 nm excitation laser line. For each v'' vibrational level the fluorescence lines were R (13) and P (15). The results were obtained using $eQq_B = -533$ MHz in $v'=32$ (Ref. 22). The given error is an estimate of the standard deviation (see text).

v''	eQq_X (MHz)	$E_{Dis}-E_v$ (cm^{-1})
26	−2518 ± 60	7317, 55
27	−2512 ± 60	7139, 46
28	−2491 ± 60	6962, 91
29	−2511 ± 50	6787, 92
30	−2523 ± 70	6614, 50
31	−2520 ± 50	6442, 68
32	−2488 ± 150	6272, 48
33	−2484 ± 50	6103, 91
34	−2426 ± 100	5937, 00
35	−2474 ± 50	5771, 78
36	−2463 ± 50	5608, 26
37	−2449 ± 50	5446, 48
38	−2437 ± 50	5286, 45
39	−2436 ± 50	5128, 20
40	−2424 ± 50	4971, 80
41	−2418 ± 70	4817, 16
42	−2407 ± 50	4664, 40
43	−2405 ± 70	4513, 60
44	−2360 ± 50	4364, 70
45	−2349 ± 50	4217, 80
46	−2348 ± 50	4072, 83
47	−2365 ± 50	3929, 92
48	−2353 ± 50	3789, 07
49	−2345 ± 50	3650, 33
50	−2296 ± 70	3513, 74
51	−2341 ± 50	3379, 32
52	−2348 ± 150	3247, 13
53	−2287 ± 50	3117, 20
54	−2261 ± 50	2989, 57
55	−2228 ± 50	2864, 30
56	−2250 ± 50	2741, 39
57	−2264 ± 150	2620, 92
58	−2243 ± 50	2502, 93
59	−2225 ± 100	2387, 45
60	−2202 ± 70	2274, 60

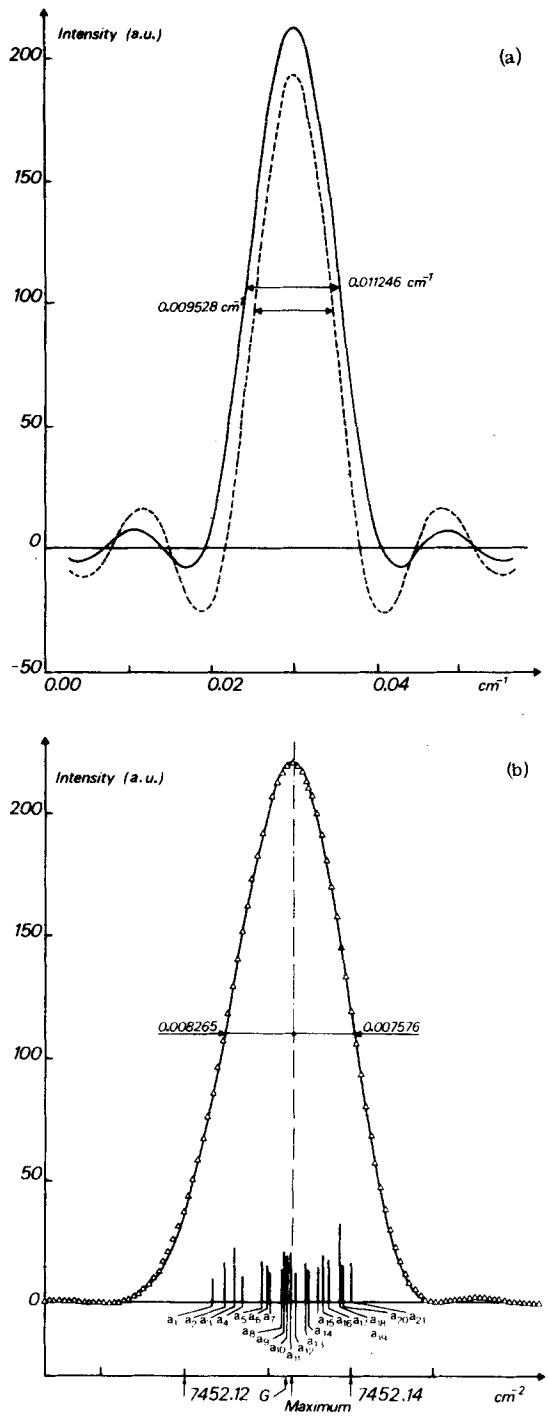

FIG. 1. Line shape of the (43-83) $P(13)$ line ($\nu_0 = 7452.133$ cm^{-1}). (a) Dashed line: calculated apparatus function = $= \sin 2\Pi(\nu - \nu_0)\delta M / 2\Pi(\nu - \nu_0)\delta M * \text{rect}\ \nu/\nu_0(\alpha^2/2)$, where $1/2\delta M = 0.00720$ cm^{-1} is the resolution limit (nonapodized as in other records used) and $\alpha = 0.15 \times 10^{-2}$ the angular radius of the entrance hole. The full width at half-maximum (FWHM) is 0.009528 cm^{-1}. Full line: Single line function (FWHM = 0.011246 cm^{-1}) convolution of the apparatus function and a Doppler broadened line (559 °K and related Doppler width = 0.00792 cm^{-1}). (b) Full line: recorded line. Half-width at half-maximum (HWHM) (red side) = 0.008275 cm^{-1}, (HWHM) (violet side) = 0.007576 cm^{-1}. Triangles: calculated line (HWHM) (red side) = 0.008239 cm^{-1}, (HWHM) (violet side) = 0.007618 cm^{-1}. $(eQq')_{43} = -558.6$ MHz, $(C_I')_{43} = 0.19$ MHz, $(eQq'')_{83} = -1557$ MHz. The center of gravity of the line (G) is 0.000616 cm^{-1} on the red side of the maximum. The intensity of the 21 hyperfine components is on the same scale as the line shape.

T generates no asymmetry. For the five vibrational levels studied in this way, we obtain the same temperature within the error bars

$$T = 579 \pm 11\ ^\circ\text{K},$$

where the error bar represents one standard deviation.

This temperature is now used to interpret all the other lines recorded under the same conditions. This high value of T is not really surprising since an important fraction of the 7 W 514.5 nm laser line was absorbed in the cell ($\simeq 10\%$).

The rather good precision obtained in the determination of and eQq'' is due to the very high signal to noise ratio of the analysed lines. Obviously if the linewidth due to hyperfine structure is smaller than the Doppler width we cannot measure ΔeQq. This happens when $|\Delta eQq| \lesssim 300$–$400$ MHz, i.e., $-900 < eQq'' < -100$ MHz. The eQq'' values obtained are outside this range.

V. EXPERIMENTAL RESULTS AND DISCUSSION

A. X state

1. Measurements

We have measured eQq_X in the X state for various vibrational levels. The results are summarized in Tables II–IV, and in Figs. 2(a) and 2(b). The indicated errors correspond to one standard deviation and in principle the error given by the temperature, the apparatus function and the SNR is taken into account. For this last one, we used Maillard's error coefficient on the maximum of the line.[18] Using various measurements of a same line with different SNR, we have seen that this error coefficient gives also a good estimate of the error on the width of the line and then on eQq''.

In Table II, we give also the results obtained previously and available in the literature. For some vibrational levels (for instance $v'' = 83$), eQq_X has been already measured in more precise experiments[13,15,16] where the hyperfine splittings were completely resolved. The agreement with our results is satisfactory.

In our computer fit, we have neglected the spin rotation constant C_I' ($C_I' \mathbf{I} \cdot \mathbf{J}$) in the X state. This is reasonable because C_I' is zero to first order in a O_g^+ state and the only measured value of C_I' is very small: $C_I' = 59$ kHz in the level $v'' = 83$.[15] Moreover, the J'' values of the transitions studied are rather weak ($J'' \leq 28$) and the linewidth produced by this term is negligible being roughly equal to $C_I' IJ''$. However, this approximation is only justified as far as the 1_g state does not perturb the X state. The effects of this perturbation are the following: it introduces an important value to C_I' which may be of the order of a few MHz; the eQq value of the perturbed levels is a linear combination of eQq_X and eQq_{1_g}.

The examination of the possible perturbed vibrational levels of the X state[11] shows we can consider that for $v'' \leq 88$, C_I' is nearly negligible and that the eQq value is not polluted by eQq_{1_g}. This is probably not the case for $v'' \geq 89$. Unfortunately, the SNR of these lines is too weak to allow the determination of two hyperfine

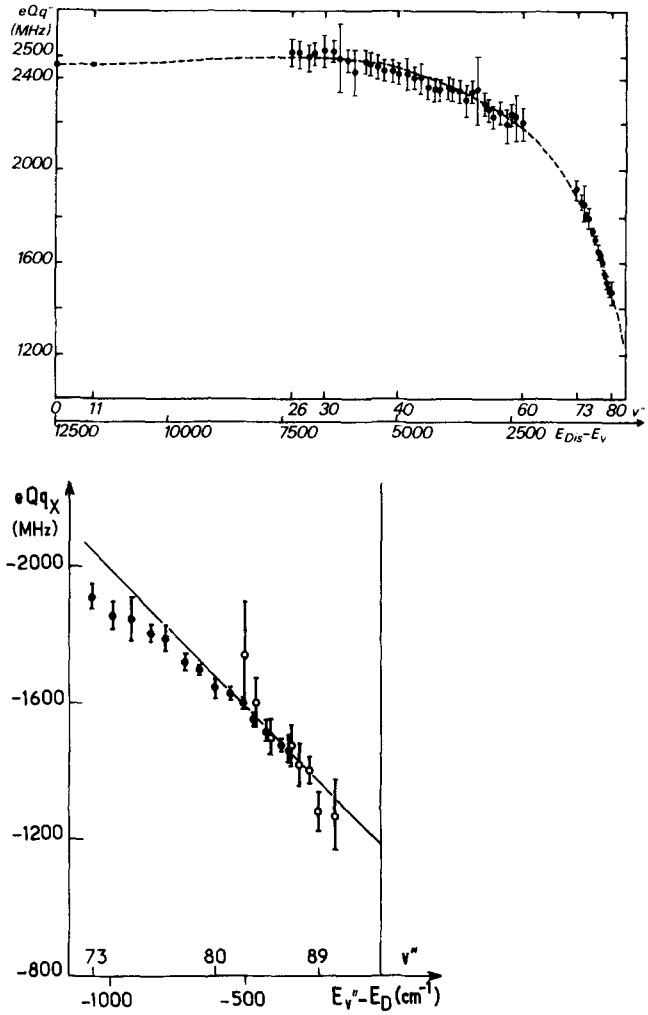

FIG. 2. eQq_X variation as a function of the vibrational energy. (a) The dashed line is an approximate curve for the guidance of the eye. In the range where no determination was made ($v'' < 26$ and $60 < v'' < 73$) the examination of the widths of the lines shows that eQq_X variation is smooth and regular with v'' following the trend shown by the dashed line. (b) eQq_X variation in the region of the dissociation limit. Black circle: measurement from the 514.5 nm excitation; open circle: measurement from the 501.7 nm excitation. The straight line is obtained from a weighted least-squares fit with $81 \leqslant v'' \leqslant 87$ points.

parameters. For these reasons, we have kept $C_I'' = 0$ in our fit and the eQq value obtained for these levels is in fact an effective one. In Table II, we have reported these effective eQq values in the range $89 \leqslant v'' \leqslant 107$. These values present a very rapid decrease followed by a large increase. These effects are surely related to perturbations by the 1_g state; As the calculated and measured eQq_{1_g} value is zero (see Sec. V C), the mixing between the two states could explain the decrease, but not the increase of eQq_X. Therefore, the most probable explanation of this increase lies in the influence of the C_I'' parameter, neglected in the fit because the value of C_I'' induced by a mixing with the $1g$ state is large and can changes sign around the perturbation.

Since the goal of this paper is to compare experimental and theoretical values of eQq_X, we must exclude from this comparison all the values of levels which are perturbed by the 1_g state and we consider as reliable only the values with $v'' \leqslant 88$. Only these values appear in Figs. 2(a) and 2(b) and are used in the extrapolation at the dissociation limit. In fact we have determined the dissociation limit value of eQq_X [noted $(eQq_X)_{DL}$] by linear extrapolation between the points corresponding to $81 \leqslant v'' \leqslant 87$ using a weighted least-squares fit and we have found

$$(eQq_X)_{DL} = -1170 \pm 40 \text{ MHz} .$$

In the perturbed region $89 \leqslant v'' \leqslant 107$, our analysis is very preliminary and must be improved. The determination of both C'' and eQq'' constants by the LIF-FTS is not impossible *a priori*, this technique been only limited by the Doppler width and the apparatus function. As an illustration of the possibilities of our method, we have measured C_I' in the excited level $v' = 71$, $J' = 55$ of the B state. Indeed the 501.7 nm laser line excites various level in the B state[11,19,29]: $v' = 61$, $J' = 10$; $v' = 62$, $J' = 27$; $v' = 64$, $J' = 40$; $v' = 67$, $J' = 50$; $v' = 70$, $J' = 54$; $v' = 71$, $J' = 55$. In the level $v' = 62$, $J' = 27$, eQq', and C_I' are well known.[14,22] Therefore, we can use for instance the fluorescence line $v' = 62$, $J' = 27 \rightarrow v'' = 83$, $J'' = 26$ or 28, to determine eQq'' in the level $v'' = 83$, C_I'' being negligible in this level. Then using the fluorescence lines $v' = 71$, $J' = 55 \rightarrow v'' = 83$, $J'' = 54$ or 56, we can measured C_I' in $v' = 71$, because eQq' may be considered as known in this level (see Sec. V D and Fig. 3). This procedure has been used for various values of v'' from 74 to 85. Finally, we find $C_I' = 3.41 \pm 0.29$ MHz, in reasonable agreement with the theoretical formula for C_I' derived in Ref. 2 [formula (17), of Ref. 2). A similar step by step procedure could be used in the perturbed region $90 \leqslant v'' \leqslant 110$; for example, we could study fluores-

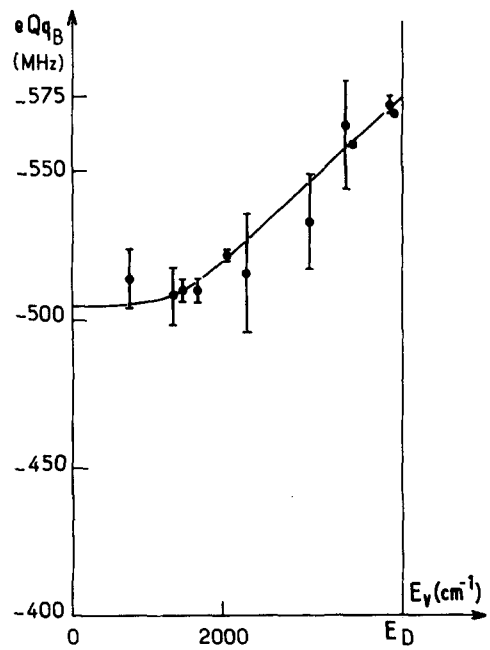

FIG. 3. eQq_B variation as a function of the vibrational energy. The full line is an approximate curve showing the trend of the eQq_B variation.

cence lines corresponding to various J'' values of the same vibrational level v'' in the X state, the hyperfine splitting produced by C_I'' being roughly proportional to $C_I'' IJ''$. In that aim we will try soon to improve the SNR in the perturbed region and then to perform a complete analysis of the perturbation both on a spectroscopic and a hyperfine structure point of view. Measurements from an iodine laser as in reference[15] would also be useful.

2. Discussion

If we limit ourselves to unperturbed levels, the results illustrated by Fig. 2(a) imply that q_X depends on the internuclear distance r. Indeed during its vibration the molecule spends most of its time in the neighborhood of the two turning points of the classical motion, r_1 in the inner wing and r_2 in the outer one. As a consequence, the q_X value in a given vibrational level mainly depends of $q_X(r_1)$ and $q_X(r_2)$. This physical intuition may be written mathematically by a formula similar to formula (9) of Ref. 2:

$$eQq_X = P_1 eQq_X(r_1) + P_2 eQq(r_2) , \tag{15}$$

where P_1 and P_2 are the weights attributed to the two turning points r_1 and r_2, respectively.

We take these weights to be proportional to the time spent by the vibrating molecule between the turning point r_1 (or r_2) and the equilibrium distance r_e:

$$P_1 = \int_{r_1}^{r_e} |\psi_v(r)|^2 \, dr \tag{15a}$$

and

$$P_2 = 1 - P_1 . \tag{15b}$$

By invoking the reasonable approximation that the major anharmonicity is due to the outer wing of the potential curve, one readily obtains

$$P_1 = \omega_v / 2\omega_e , \tag{16}$$

where ω_e is the vibrational quantum near the bottom of the well and ω_v is the spacing of vibrational levels around the level v. Some values of P_2 are given in Table II.

Near the bottom of the X state potential well, the vibrational amplitude of the molecule is weak and the LCAO calculations are valid in principle. Hence in formula (15), we have $eQq_X(r_1) \simeq eQq_X(r_2) \simeq -2293$ MHz. This is in rather good agreement with the experimental results since we obtain $-2400 \leq eQq_X \leq -2500$ MHz in a large region of the X state corresponding to $0 \leq v'' \leq 42$ and $2.3 \leq r \leq 3.3$ Å.

When one moves to the dissociation limit, P_2 tends toward 1 as can be seen from formulas (16) and (15b), and $eQq_X(r_2)$ tends to the values calculated with the separated atoms basis set. Following the results of Table I, eQq_X must tend to -1146 MHz close to the dissociation limit. Our experimental value is -1170 ± 40 MHz in good agreement with our theory.

We could use formula (15) to fit the results corresponding to $73 \leq v'' \leq 83$ with an additional hypothesis: $eQq(r_1) = eQq(r_e) = -2450$ MHz. This seems reasonable since for these levels, $r_1 \approx 2.3$ Å is not very different of $r_e = 2.65$ Å. Then we can deduce $eQq(r_2)$ from formula (15). The results are also reported in Table II. This model is rather rough and must not be considered as perfect since $eQq(r_1)$ may be slightly different of $eQq(r_e)$. However, Table II shows that the transition between the LCAO region and the separated atom region, takes place mainly between 3.5 and 4.5 Å.

B. O_g^+ state

In this state we have studied only two vibrational levels ($v'' = 1$ and 2). The fluorescence was obtained on the same record as in Fig. 1(b), the exciting laser line being also at 514.5 nm. The SNR on these transitions corresponding to B ($v' = 43$, $J' = 12$ and 16) $\rightarrow O_g^+(v'', J'')$ is rather low. The intensity of the most intense line is 1000 times weaker than for the line shown in Fig. 1.

As for the X state and for the same reasons we neglect in our fit the spin rotation constant C_I'. We do not observe any significant difference between the two studied vibrational levels. We obtained for the two averaged HWHM of the lines

0.0092 ± 0.0022 cm^{-1} (red side)

and

0.0136 ± 0.0024 cm^{-1} (violet side) .

This leads to

$$eQq_{O_g^+} = +1030 \pm 190 \text{ MHz} .$$

In fact a negative value of $eQq_{O_g^+}$ of the order of -2200 MHz would give the same FWHM, but the asymmetry would be the inverse (larger red side).

The agreement between the measured $eQq_{O_g^+}$ and the theoretical value of Table I ($+1146$ MHz) is good. For this state the LCAO and the separated atom eigenfunctions give the same result. However, we are in the region where the separated atoms eigenfunctions are valid since $r_e = 4.6$ Å for the O_g^+ state.[1,11]

C. 1_g state

In this state only four vibrational levels ($v'' = 0$, 1, 3, and 4) were analyzed. The measurements are made on the same record as on Fig. 1(b). The transitions are issued from the levels $v' = 43$, $J' = 12$ and 16 of the B state. The intensity of the studied lines is about $\frac{1}{200}$ to $\frac{1}{500}$ the intensity of the line shown in Fig. 1(b). In a 1_g state, the spin rotation constant C_I does not vanish at first order as for a O_g^+ state. This constant may be calculated *ab initio* using the separated atom basis set. The calculation is given in Appendix B and the result is

$$(C_I)_{1g} = \frac{414}{2J''(J''+1)} \text{ MHz} . \tag{17}$$

This value is introduced in the fit, but C_I has a small effect and the final result would not be significantly changed if C_I were to be varied by $\pm 50\%$ from its theoretical value.

For a given transition we are able to measure only the parameter $(eQq_{1g})_{eff}$. However, ϵ in formula (5)

TABLE V. eQq values in the B state of $^{127}I_2$. The error bars less than 1 MHz are not given. We used $eQq_X = -2452.6$ in $v'' = 0$, $eQq_X = -2452 \pm 3$ in $v'' = 1$, and $eQq_Q = -2452 \pm 10$ in $v'' = 3$ and 5.

transition $v'-v''$	ΔeQq (MHz)	eQq_B	r_1 (Å)	r_2 (Å)	P_2	$E_{v''}$ (cm^{-1})	$eQq_B(r_2)$
6→3[a]	1938	−514 ± 10	2.84	3.29	0.535	785	−522
11→5[b]	1944.0	−508 ± 10	2.78	3.44	0.575	1341	−510
12→0[c]		−510 ± 4	2.77	3.45	0.582	1448	−514
14→0[e]		−510 ± 4	2.76	3.52	0.596	1655	−513
18→0[d]	1930.5 ± 5	−522 ± 2	2.73	3.62	0.626	2047	−532
21→1[e]	1936 ± 17	−516 ± 2	2.72	3.70	0.649	2321	−522
32→0[e]	1920 ± 16	−533 ± 16	2.68	4.02	0.738	3172	−543
40→0[e]	1988 ± 16	−565 ± 16	2.66	4.42	0.804	3634	−580
43→0[f]	1894.0	−558.6	2.65	4.47	0.828	3773	−570
58→1[g]	1880.2	−572 ± 33	2.63	5.50	0.928	4221	−577
62→0[f]	1883.5	−569.2	2.63	5.95	0.948	4383	−573

[a]Reference 20.
[b]Reference 21.
[c]References 11 and 25.
[d]Reference 26.
[e]Reference 22.
[f]Reference 14.
[g]Reference 23.

changes when one goes from a Q line ($\epsilon = -1$) to an R or P line ($\epsilon = +1$). We have observed no significant variation of $(eQq_{1_g})_{eff}$ between R or P lines and Q lines. We deduce from this comparison that

$$(eQq_1)_{1_g} = 0 \pm 150 \text{ MHz} .$$

Moreover, we observe no significant variation between the four vibrational levels we have studied. For all of them, we obtain

$$eQq_{1_g} = -30 \pm 70 \text{ MHz} .$$

The precision on this measurement is not very high because in the transitions $B \rightarrow 1_g$, $\Delta eQq = eQq_B - eQq_{1_g}$ is small and that in this case, the FWHM of the lines (0.01265 ± 0.00023 cm^{-1}) is mainly due to the apparatus function convoluted by the Doppler width (0.011246 cm^{-1}).

This result for eQq_{1_g} is in reasonable agreement with the theoretical eQq_{1_g} value obtained with the separated atom basis set. This is not surprising since the equilibrium distance in the 1_g state is rather large[11]: $r_e \simeq 4.3$ Å.

D. B state

No eQq measurements were made in the B state by the LIF–FTS method. However the hyperfine structure of the B state has been extensively measured by Doppler free spectroscopy using fixed frequency lasers[14,20–24] or tunable lasers.[25–27] The aim in this paragraph is to compare the results available in the literature with our theory.

Generally in such experiments, the precisely measured parameters are the difference between the hyperfine parameters of the excited state and those of the ground state. The available parameter is $\Delta eQq = eQq_B - eQq_X$. It is possible to determine both eQq_B and eQq_X only if the J' value of the excited state is low ($J' \leq 15$). Table V gives the ΔeQq parameters measured by various authors. To extract eQq_B we must know eQq_X for the various studied transitions. Many transitions involve the $v'' = 0$ level of the X state, where eQq_X is known with a good accuracy: $eQq_X = -2452.6$ MHz. There is no measurements in the X state between $v'' = 0$ and $v'' = 11$ (Table II). Since the eQq_X variation in this region seems very smooth [see Fig. 2(a)] we have used $eQq_X = -2452 \pm 3$ MHz in the level $v'' = 1$, and $eQq_X = -2452 \pm 10$ MHz in the levels $v'' = 3$ and $v'' = 5$, in Table V to calculate eQq_B.

The variation of eQq_B as a function of the vibrational energy is shown in Fig. 3. In this figure we have drawn a curve $eQq_B = f(E_v)$ by approximate interpolation between the experimental results. This curve may be extrapoled to -574 ± 3 MHz at the dissociation limit and to -505 ± 15 MHz near the bottom of the well.

As in the X state, eQq_B in a given vibrational level may be approximated by the formula

$$eQq_B(E_v) = P_1 eQq_B(r_1) + P_2 eQq_B(r_2) . \quad (18)$$

The values of the two turning points r_1 and r_2 and of P_2 are also given in Table V for the levels studied.

The theoretical eQq_B values are the same in the two basis sets, LCAO and separated atoms, as it is shown in Table I. Hence eQq_B should be constant and independent of the vibrational energy. This is approximately true since the observed variations of eQq_B are smaller than 15%. Near the dissociation limit the agreement between the theoretical value (573 MHz) and the experimental one (574 ± 3 MHz) is excellent, but at the bottom of the well, it is not good (505 ± 15 MHz as compared to 573 MHz). This is not surprising: at very large internuclear distance the eigenfunction of the molecule must be a product of separated atom eigenfunction, but even at the equilibrium distance, the LCAO eigenfunction is only a rough approximation.

We can also use formula (18) to calculate $eQq_B(r_2)$ as a function of r_2, assuming that $eQq_B(r_1) \simeq -505$ MHz. This last assumption seems reasonable because r_1 varies merely from 2.84 to 2.63 Å. The $eQq_B(r_2)$ values thus obtained are reported in Table V. They show the separated atom basis set is very good above an internuclear distance of about 4.5 Å.

TABLE VI. Comparison between experimental and theoretical results at short and long range internuclear distance.

	eQq From LCAO (in MHz)	Internuclear distance[a] (Å)	Experimental results (MHz)	eQq From SA (MHz)	Internuclear distance[a] (Å)	Experimental results (MHz)
$X\,^1\Sigma_g^+$	−2293	2.5 to 3 Å	−2452 ± 10	−1146	∞	−1170 ± 40
$^3\Sigma_{O_g^+}^-$	+1146			+1146	4.5 to 5 Å	+1030 ± 190
$^3\Pi_{1_g}$	$eQq_{1_g} = -579$ $eQq_{\perp 1_g} = -1404$			0 0	4 to 5 Å	0 ± 150 30 ± 50
$B\,^3\Pi_{O_u^+}$	−573	2.7 to 3.5 Å	−505 ± 15	−573	∞	−574 ± 3

[a]In this table we give the internuclear distance, where eQq has been measured.

VI. CONCLUSION

From our experiments and some other results available in the literature, we are able to predict the variation of the quadrupole electric constant eQq in the B and X states as a function of the vibrational energy. In the two recently discovered O_g^+ and 1_g states, which are weakly bound at large internuclear distance, we have also measured eQq parameters. All these results have been interpreted using *ab initio* calculations. Table VI summarizes the rather good agreement between the theory and experiment. In fact to our knowledge it is the first time that the quadrupole hyperfine constant has been studied close to a dissociation limit and in a so wide range of vibrational levels. This has been possible thanks to the precise and very large amount of informations given by the LIF–FTS. Our approach is quite general and can be applied to any molecular state close to a dissociation limit. Moreover we have shown that the eQq value may be considered as a probe of the molecular eigenfunction. For example, from our experimental results, we are able to predict that, in the X and B states, the separated atom eigenfunctions are a good approximation above an internuclear distance of about 4 or 4.5 Å.

ACKNOWLEDGMENTS

The authors wish to thank Professor R. W. Field and Professor J. C. Lehmann for many helpful and stimulating discussions and suggestions.

APPENDIX A: CALCULATION OF $q_{\perp 1_g}$ IN THE LCAO APPROXIMATION

We have to calculate

$$q_{\perp 1_g} = 2\langle \Omega = +1_g | \sum_e V_2^2(a, e) | \Omega = -1_g \rangle . \tag{19}$$

The electronic configuration of the 1_g states is $\sigma_g^2 \pi_u^3 \pi_g^4 \sigma_u^1$. One goes from the $+1_g$ state to the -1_g state by changing an orbital $\Pi_u = +1$ to an orbital $\Pi_u = -1$. As a result, in formula (19), the summation over the electrons is reduced to one term $V_2^2(a, e_1)$, where e_1 is the electron in the orbital $\pi_u = -1$ or $\pi_u = +1$. Therefore,

$$q_{\perp 1_g} = 2\langle \pi_u = +1 | V_2^2(a, e_1) | \pi_u = -1 \rangle , \tag{20}$$

$$|\pi_u = +1\rangle = (1/\sqrt{2})(|l = 1\, m_l = +1\rangle_a + |l = 1\, m_l = +1\rangle_b) , \tag{21}$$

$$|\pi_u = -1\rangle = (1/\sqrt{2})(|l = 1\, m_l = -1\rangle_a + |l = 1\, m_l = -1\rangle_b) , \tag{22}$$

$$q_{\perp 1_g} = 2\tfrac{1}{2}{}_a\langle l = 1\, m_l = +1 | V_2^2(a, e_1) | l = 1\, m_l = -1\rangle_a . \tag{23}$$

We can now use the Wigner–Eckart theorem

$$q_{\perp 1_g} = (-1)^{1-1} \begin{pmatrix} 1 & 2 & 1 \\ -1 & 2 & -1 \end{pmatrix}_a \langle 5P \| V^2(a, e_1) \| 5P \rangle_a . \tag{24}$$

We also have

$$q_{1_g} = \tfrac{1}{2} q_{511} = {}_a\langle l = 1\, m_l = +1 | V_0^2(a, e_1) | l = 1,\ m_l = 1\rangle_a , \tag{25}$$

$$q_{1_g} = (-1)^{1-1} \begin{pmatrix} 1 & 2 & 1 \\ -1 & 0 & 1 \end{pmatrix}_a \langle 5P \| V^2(a, e_1) \| 5P \rangle_a , \tag{26}$$

and we deduce

$$q_{\perp 1_g} = q_{1_g}\sqrt{6} = -1404 \text{ MHz} .$$

Formula (5) of Sec. II can be written

$$(eQq)_{\text{eff}} = eQq_{1_g}\left(1 - \frac{3}{J(J+1)}\right) - 3\epsilon eQq_{1_g} , \tag{27}$$

with

$$eQq_{1_g} = -573 \text{ MHz} .$$

APPENDIX B: CALCULATION OF THE DIRECT SPIN ROTATION COUPLING CONSTANT $C_I \mathbf{I}\cdot\mathbf{J}$ IN THE 1_g STATE

This term must be evaluated at the bottom of the 1_g state potential well, at a rather large internuclear distant (4 to 5 Å) when the separated atom basis set is a good approximation. As eigenfunction we use

$$|1_g\rangle = (1/\sqrt{2})(|\tfrac{3}{2}\,\tfrac{3}{2}\rangle_a |\tfrac{3}{2} - \tfrac{1}{2}\rangle_b - |\tfrac{3}{2} - \tfrac{1}{2}\rangle_a |\tfrac{3}{2}\,\tfrac{3}{2}\rangle_b) . \tag{28}$$

The direct spin rotation coupling constant C_I is due to the magnetic dipole Hamiltonian of the molecule. This interaction can be written[23]

$$\begin{aligned} H_{\text{MD}} &= H_{\text{MD}}(a) + H_{\text{MD}}(b) , \\ H_{\text{MD}}(a) &= \sum_q \sum_e (-1)^q Q_q^1(I_a)\, V_{-q}^1(a, e) . \end{aligned} \tag{29}$$

The matrix elements of H_{MD} are easy to calculate by standard method[19,28]

$$\begin{aligned} &\langle \Omega J(I_a I_b) IF | H_{\text{MD}} | \Omega J(I_a I_b) IF \rangle \\ &= (-1)^{1+I_a+I_b+F+2I+2J} 2 f_1(a, \Omega, \Omega)(2I+1)(2J+1) \\ &\times \begin{pmatrix} J & 1 & J \\ -\Omega & 0 & \Omega \end{pmatrix} \begin{Bmatrix} I_b & I_a & I \\ 1 & I & I_a \end{Bmatrix} \begin{Bmatrix} F & I & J \\ 1 & J & I \end{Bmatrix} , \end{aligned} \tag{30}$$

where

$$f_1(a, \Omega, \Omega) = (-1)^{\Omega} \langle \Omega v | \sum_e V_0^1(a, e) | \Omega v \rangle \quad (31)$$

Finally, we find

$$\langle \Omega J(I_a I_b) IF | H_{MD} | \Omega J(I_a I_b) IF \rangle = \tfrac{1}{2} C_I [F(F+1) - (J(J+1) - I(I+1)] , \quad (32)$$

where

$$C_I = + \langle 1_g | \sum_e V_0^1(a, e) | 1_g \rangle / J(J+1) . \quad (33)$$

Using expression (28) for the 1_g state, we obtain

$$C_I = [1/2J(J+1)] [{}_a\langle \tfrac{3}{2} \tfrac{3}{2} | V_0^1(a, e) | \tfrac{3}{2} \tfrac{3}{2} \rangle_a + {}_a\langle \tfrac{3}{2} -\tfrac{1}{2} | V_0^1(a, e) | \tfrac{3}{2} -\tfrac{1}{2} \rangle_a] . \quad (34)$$

The Wigner–Eckart theorem can now be applied, giving

$${}_a\langle \tfrac{3}{2} \tfrac{3}{2} | V_0^1(a, e) | \tfrac{3}{2} \tfrac{3}{2} \rangle_a = (-1)^{3/2-3/2} \begin{pmatrix} \frac{3}{2} & 1 & \frac{3}{2} \\ -\frac{3}{2} & 0 & \frac{3}{2} \end{pmatrix} \times \langle {}^2P_{3/2} \| V^1(a, e) \| {}^2P_{3/2} \rangle , \quad (35)$$

$${}_a\langle \tfrac{3}{2} -\tfrac{1}{2} | V_0^1(a, e) | \tfrac{3}{2} -\tfrac{1}{2} \rangle_a = (-1)^{3/2+1/2} \begin{pmatrix} \frac{3}{2} & 1 & \frac{3}{2} \\ \frac{1}{2} & 0 & -\frac{1}{2} \end{pmatrix} \times \langle {}^2P_{3/2} \| V^1(a, e) \| {}^2P_{3/2} \rangle . \quad (36)$$

The reduced matrix element $\langle {}^2P_{3/2} \| V^1(a, e) \| {}^2P_{3/2} \rangle$ can easily be related to the hyperfine magnetic dipole parameter $a_{3/2}$ in the $^{127}I\ {}^2P_{3/2}$ state

$$\langle {}^2P_{3/2} \| V^1(a, e) \| {}^2P_{3/2} \rangle = \sqrt{15}\, a_{3/2} . \quad (37)$$

We finally obtain

$$C_I = a_{3/2} / 2J(J+1) .$$

$a_{3/2}$ is known[5]: $a_{3/2} = 827$ MHz, and thus $C_I = 413.5/J(J+1)$ MHz.

[1]R. Bacis, S. Churassy, R. W. Field, J. B. Koffend, and J. Vergès, (a) 33rd Symposium on Molecular Spectroscopy, Communication MF2, June 1978 (unpublished); (b) J. Chem. Phys. **72**, 34 (1980).

[2]J. Vigué, M. Broyer, and J. C. Lehmann, Phys. Rev. Lett. **42**, 883 (1979).

[3]C. H. Townes and A. L. Schawlow, *Microwave Spectroscopy* (McGraw-Hill, New York, 1955).

[4]W. Gordy and R. L. Cook, *Microwave Molecular Spectra* (Interscience, New York, 1970).

[5]V. Jaccarino, J. G. King, R. A. Satten, and H. H. Stroke, Phys. Rev. **94**, 1798 (1954).

[6]R. S. Mulliken, J. Chem. Phys. **55**, 288 (1971).

[7]C. Effantin, thèse (Lyon, 1976) (unpublished); C. Effantin, R. Bacis, and J. d'Incan, Phys. Rev. A **15**, 1053 (1977).

[8]E. P. Gordeev, S. Y. Umansky, and A. J. Voronin, Chem. Phys. Lett. **23**, 524 (1973).

[9]R. S. Mulliken, Phys. Rev. **46**, 549 (1934).

[10]A. R. Edmonds, *Angular Momentum in Quantum Mechanics* (Princeton U.P., Princeton, N.J., 1967).

[11](a) S. Churassy, thèse (Lyon, 1979) (unpublished); (b) S. Churassy, R. Bacis, R. W. Field, F. Martin, and J. Vergès (unpublished).

[12]J. Vergès, J. d'Incan, C. Effantin, D. J. Greenwood, and R. F. Barrow, J. Phys. B **12**, L301 (1979).

[13]J. B. Koffend, Ph.D. thesis (M.I.T., Cambridge, Mass., 1978) (unpublished).

[14]J. Camy, J. Vigué, C. Bordé, and J. P. Descoubes (unpublished).

[15]J. B. Koffend, S. Goldstein, R. Bacis, R. W. Field, and S. Ezekiel, Phys. Rev. Lett. **41**, 1040 (1978).

[16]R. P. Hackel and S. Ezekiel, Phys. Rev. Lett. **42**, 1736 (1979).

[17]X. Muenter and X. Yokoseki (unpublished); and private communication.

[18]J. P. Maillard, thèse (Paris, 1973) (unpublished).

[19](a) M. Broyer, thèse (Paris VI, 1977) (unpublished). (b) M. Broyer, J. Vigué, and J. C. Lehmann, J. Phys. (Paris) **39**, 591 (1978).

[20]G. A. Hanes, J. Lapierre, P. R. Bunker, and K. C. Shotton, J. Mol. Spectrosc. **39**, 506 (1971).

[21]B. M. Landsberg, Chem. Phys. Lett. **43**, 102 (1976).

[22]M. D. Levenson and A. L. Schawlow, Phys. Rev. A **6**, 10 (1972).

[23]H. J. Foth and F. Spieweck, Chem. Phys. Lett. **65**, 347 (1979).

[24]L. A. Hackel, K. H. Coselton, S. G. Kukolich, and S. Ezekiel, Phys. Rev. Lett. **35**, 568 (1973).

[25]S. Churassy, G. Grenet, M. L. Gailard, and R. Bacis, Opt. Commun. **30**, 41 (1979).

[26]H. Brand, H. H. Schulz, and A. Steudel, Phys. Lett. A **63**, 285 (1977).

[27]B. Couillaud and A. Ducasse, Opt. Commun. **13**, 398 (1975).

[28]J. Vigué, M. Broyer, and J. C. Lehmann, J. Phys. (Paris) (to be published).

[29]S. Gerstenkorn and P. Luc, J. Mol. Spectrosc. **77**, 310 (1979).